**Article:**
Tsiligiannis, Epameinondas, Wu, Rongrong, Lee, Ben H. et al. (27 more authors) (2022) A Four Carbon Organonitrate as a Significant Product of Secondary Isoprene Chemistry. Geophysical Research Letters. e2021GL097366. ISSN 0094-8276

https://doi.org/10.1029/2021GL097366

Geophysical Research Letters

RESEARCH LETTER
10.1029/2021GL097366

# A Four Carbon Organonitrate as a Significant Product of Secondary Isoprene Chemistry

**Epameinondas Tsiligiannis[1], Rongrong Wu[2,3], Ben H. Lee[4], Christian Mark Salvador[1,5], Michael Priestley[1], Philip T. M. Carlsson[2], Sungah Kang[2], Anna Novelli[2], Luc Vereecken[2], Hendrik Fuchs[2], Alfred W. Mayhew[6], Jacqueline F. Hamilton[6], Peter M. Edwards[6], Juliane L. Fry[7,8], Bellamy Brownwood[7], Steven S. Brown[9,10], Robert J. Wild[9,11], Thomas J. Bannan[12], Hugh Coe[12], James Allan[12], Jason D. Surratt[13], Asan Bacak[12,14], Paul Artaxo[15], Carl Percival[16], Song Guo[3], Min Hu[3], Tao Wang[17], Thomas F. Mentel[2], Joel A. Thornton[4], and Mattias Hallquist[1]**

[1]Department of Chemistry and Molecular Biology, University of Gothenburg, Gothenburg, Sweden, [2]Institute of Energy and Climate Research, IEK-8: Troposphere, Forschungszentrum Jülich GmbH, Jülich, Germany, [3]State Key Joint Laboratory of Environmental Simulation and Pollution Control, International Joint Laboratory for Regional Pollution Control, Ministry of Education (IJRC), College of Environmental Sciences and Engineering, Peking University, Beijing, China, [4]Department of Atmospheric Sciences, University of Washington, Seattle, WA, USA, [5]Now at Balik Scientist Program, Department of Science and Technology – Philippine Council for Industry, Energy and Emerging Technology Research and Development, Taguig, Philippines, [6]Wolfson Atmospheric Chemistry Laboratories, Department of Chemistry, University of York, York, UK, [7]Department of Chemistry, Reed College, Portland, OR, USA, [8]Now at Department of Meteorology and Air Quality, Wageningen University, Wageningen, The Netherlands, [9]NOAA Chemical Sciences Laboratory, Boulder, CO, USA, [10]Department of Chemistry, University of Colorado, Boulder, CO, USA, [11]Now at Institute for Ion and Physics, University of Innsbruck, Innsbruck, Austria, [12]Centre for Atmospheric Science, School of Earth and Environmental Science, University of Manchester, Manchester, UK, [13]Department of Environmental Sciences and Engineering, Gillings School of Global Public Health, The University of North Carolina at Chapel Hill, Chapel Hill, NC, USA, [14]Now at Turkish Accelerator & Radiation Laboratory, Ankara University Institute of Accelerator Technologies, Atmospheric and Environmental Chemistry Laboratory, Gölbaşı Campus, Ankara, Turkey, [15]Institute of Physics, University of Sao Paulo, Sao Paulo, Brazil, [16]Jet Propulsion Laboratory, Pasadena, CA, USA, [17]Department of Civil and Environmental Engineering, Hong Kong Polytechnic University, Hong Kong, China

**Abstract** Oxidation of isoprene by nitrate radicals ($NO_3$) or by hydroxyl radicals (OH) under high $NO_x$ conditions forms a substantial amount of organonitrates (ONs). ONs impact $NO_x$ concentrations and consequently ozone formation while also contributing to secondary organic aerosol. Here we show that the ONs with the chemical formula $C_4H_7NO_5$ are a significant fraction of isoprene-derived ONs, based on chamber experiments and ambient measurements from different sites around the globe. From chamber experiments we found that $C_4H_7NO_5$ isomers contribute 5%–17% of all measured ONs formed during nighttime and constitute more than 40% of the measured ONs after further daytime oxidation. In ambient measurements $C_4H_7NO_5$ isomers usually dominate both nighttime and daytime, implying a long residence time compared to $C_5$ ONs which are removed more rapidly. We propose potential nighttime sources and secondary formation pathways, and test them using a box model with an updated isoprene oxidation scheme.

**Plain Language Summary** Isoprene is the most abundant non-methane trace gas emitted from vegetation in the atmosphere. Isoprene reacts with different oxidants forming numerous multifunctional products that affect both ozone and particulate matter concentrations via secondary organic aerosol formation. Day and nighttime isoprene oxidation under polluted conditions with high levels of nitrogen oxides ($NO_x$) produces nitrogen containing species. Here, we used state-of-the-art instrumentation to measure the isoprene-derived nitrogen-containing species, both in laboratory experiments and at six field sites around the globe. To support our interpretation, we apply a recently developed model for nighttime isoprene chemistry. We have identified a dominant nitrated product(s) in our experiments and with a significant ambient contribution both during day and nighttime. Key features of this species are its secondary formation from primary products and its relatively long lifetime under ambient conditions, explaining its accumulation in the atmosphere. Thus, it can be an important marker for the influence of $NO_x$ on isoprene oxidation.

**Key Points:**

- The $C_4H_7NO_5$ isomers are major secondary products of isoprene oxidation during nighttime and daytime in $NO_x$-influenced regions
- The $C_4H_7NO_5$ isomers are multi-generational products from several $C_5$ compounds that accumulate in the atmosphere
- $C_4H_7NO_5$ as a dominant isoprene-derived species, can be important for the formation of ozone

**Supporting Information:**

Supporting Information may be found in the online version of this article.

**Correspondence to:**

M. Hallquist and J. A. Thornton,
hallq@chem.gu.se;
thornton@atmos.washington.edu

**Citation:**

Tsiligiannis, E., Wu, R., Lee, B. H., Salvador, C. M., Priestley, M., Carlsson, P. T. M., et al. (2022). A four carbon organonitrate as a significant product of secondary isoprene chemistry. *Geophysical Research Letters*, *49*, e2021GL097366. https://doi.org/10.1029/2021GL097366

Received 6 DEC 2021
Accepted 30 APR 2022

**Author Contributions:**

**Conceptualization:** Epameinondas Tsiligiannis, Ben H. Lee, Thomas F. Mentel, Joel A. Thornton, Mattias Hallquist
**Data curation:** Epameinondas Tsiligiannis, Rongrong Wu, Ben H. Lee, Christian Mark Salvador, Michael Priestley, Philip T. M. Carlsson, Sungah Kang, Juliane L. Fry, Bellamy Brownwood, Robert J. Wild, Thomas J. Bannan, Asan Bacak
**Formal analysis:** Epameinondas Tsiligiannis

**Investigation:** Epameinondas Tsiligiannis, Rongrong Wu, Ben H. Lee, Christian Mark Salvador, Michael Priestley, Philip T. M. Carlsson, Sungah Kang, Anna Novelli, Luc Vereecken, Hendrik Fuchs, Alfred W. Mayhew, Jacqueline F. Hamilton, Peter M. Edwards, Juliane L. Fry, Bellamy Brownwood, Robert J. Wild, Thomas J. Bannan, Asan Bacak
**Project Administration:** Anna Novelli, Hendrik Fuchs, Juliane L. Fry, Steven S. Brown, Hugh Coe, James Allan, Jason D. Surratt, Paul Artaxo, Carl Percival, Song Guo, Min Hu, Tao Wang, Thomas F. Mentel, Joel A. Thornton, Mattias Hallquist
**Supervision:** Anna Novelli, Hendrik Fuchs, Juliane L. Fry, Steven S. Brown, Hugh Coe, James Allan, Jason D. Surratt, Paul Artaxo, Carl Percival, Song Guo, Min Hu, Tao Wang, Thomas F. Mentel, Joel A. Thornton, Mattias Hallquist
**Validation:** Epameinondas Tsiligiannis, Rongrong Wu, Ben H. Lee, Philip T. M. Carlsson, Anna Novelli, Luc Vereecken, Hendrik Fuchs, Thomas F. Mentel, Joel A. Thornton, Mattias Hallquist
**Visualization:** Epameinondas Tsiligiannis, Philip T. M. Carlsson
**Writing – original draft:** Epameinondas Tsiligiannis
**Writing – review & editing:** Epameinondas Tsiligiannis, Rongrong Wu, Ben H. Lee, Christian Mark Salvador, Michael Priestley, Philip T. M. Carlsson, Sungah Kang, Anna Novelli, Luc Vereecken, Hendrik Fuchs, Alfred W. Mayhew, Jacqueline F. Hamilton, Peter M. Edwards, Juliane L. Fry, Bellamy Brownwood, Steven S. Brown, Robert J. Wild, Thomas J. Bannan, Hugh Coe, James Allan, Jason D. Surratt, Asan Bacak, Paul Artaxo, Carl Percival, Song Guo, Min Hu, Tao Wang, Thomas F. Mentel, Joel A. Thornton, Mattias Hallquist

## 1. Introduction

Isoprene dominates biogenic non-methane hydrocarbon emissions, contributing around 50%, followed by monoterpenes, 15%, and sesquiterpenes, 3% (Guenther et al., 2012). Isoprene reacts mainly with hydroxyl radicals (OH), ozone ($O_3$), or nitrate radicals ($NO_3$) (Wennberg et al., 2018), influencing surface ozone concentrations and secondary organic aerosol (SOA) formation. SOA is a major component of submicron-sized tropospheric aerosol (Shrivastava et al., 2017) and affects human health and the climate (Glasius & Goldstein, 2016; Hallquist et al., 2009).

The oxidation of isoprene by OH radicals under low and high $NO_x$ conditions has been studied extensively (D'Ambro et al., 2017; Kleindienst et al., 2007; Kroll et al., 2005; L. Lee et al., 2014; Novelli et al., 2020; Peeters et al., 2014; Schwantes et al., 2019; Thornton et al., 2020; Wennberg et al., 2018) compared to $NO_3$-initiated oxidation (Kwan et al., 2012; Ng et al., 2008; Schwantes et al., 2015; Vereecken et al., 2021; Wennberg et al., 2018; Wu et al., 2021; Zhao et al., 2021). $NO_3$ is formed during nighttime from the reaction of nitrogen dioxide ($NO_2$) with ozone. Oxidation initiated by $NO_3$ radicals leads to significant formation of organonitrates (ONs) which add to the ONs produced during daytime oxidation under high $NO_x$ conditions (Hamilton et al., 2021; Kiendler-Scharr et al., 2016). ONs can act both as a reservoir and as a permanent sink of $NO_x$ (Kenagy et al., 2020; Kiendler-Scharr et al., 2016), and can contribute to SOA formation (Bryant et al., 2020; Fry et al., 2018; Kiendler-Scharr et al., 2016; Lee et al., 2016; Xu et al., 2021; Zaveri et al., 2020). Investigating isoprene-originated ONs formation is necessary to understand isoprene's effects on atmospheric $NO_x$, $HO_x$ and ozone formation (Li et al., 2019; Schwantes et al., 2020; Vasquez et al., 2020).

The dominant gas phase nitrated oxidation products from isoprene + $NO_3$ include compounds like isoprene nitrooxy hydroperoxides (INP) ($C_5H_9NO_5$), dihydroxy nitrates (IDHN) ($C_5H_9NO_5$), carbonyl nitrates (ICN) ($C_5H_7NO_4$), hydroxy nitrates (IHN) ($C_5H_9NO_4$), and hydroxy hydroperoxy nitrates (IHPN) ($C_5H_9NO_6$), among others (Schwantes et al., 2015; Vereecken et al., 2021; Wennberg et al., 2018; Wu et al., 2021). These compounds have also been observed in the ambient atmosphere (Lee et al., 2016; Schwantes et al., 2015; Xu et al., 2021; Ye et al., 2021).

To provide new insights into this important nitrate-isoprene chemistry, an extensive experimental campaign focusing on isoprene oxidation by $NO_3$ was performed in the large atmospheric simulation chamber SAPHIR in 2018. In this study we focus on the formation and fate of the isomers of one of the most ubiquitously detected ONs, $C_4H_7NO_5$, and how their atmospheric fate changes between night and daytime. The experimental findings are linked to our observations of these compounds around the globe and chemical mechanisms are proposed to support our observations.

## 2. Materials and Methods

All experimental studies and field observations in this study utilized a high resolution time-of-flight chemical ionization mass spectrometer (Aerodyne Research Inc., hereafter CIMS) to measure nitrated organic products, using iodide as the primary reagent ion (B. H. Lee et al., 2014). The CIMS was deployed for simulation chamber experiments within a comprehensive study on nighttime isoprene chemistry, for dedicated flow reactor studies, and at several field campaign sites providing diurnal concentration profiles of selected organic nitrates.

The comprehensive nighttime isoprene chemistry study was conducted in August 2018 in the atmospheric simulation chamber SAPHIR (Section S1 in Supporting Information S1) (Fuchs et al., 2017; Rohrer et al., 2005) at Forschungszentrum Jülich, Germany (Brownwood et al., 2021; Dewald et al., 2020; Vereecken et al., 2021; Wu et al., 2021). One goal of the campaign was to explore different oxidation regimes by applying conditions enhancing the contribution of different reaction pathways (i.e., $RO_2$ + $RO_2$, $RO_2$ + $HO_2$ or unimolecular $RO_2$). Nevertheless, the dominant loss of $RO_2$ were the reactions with $HO_2$ or $NO_3$, as detailed in a previous manuscript (Brownwood et al., 2021). Here we focus our analysis on four selected experiments: one experiment enhancing $HO_2$ by propene ozonolysis (exp. 1), one favoring the $RO_2$ + $RO_2$ pathway (exp. 2), and two experiments in which a nighttime to daytime transition was achieved by opening the roof of the chamber after the oxidation products of isoprene and $NO_3$ had accumulated (exp. 3 & 4, Table S1 in Supporting Information S1). The daytime chemistry favored either oxidation by OH in exp. 3, or only photolysis by scavenging OH by CO addition in exp. 4. Exp. 3 favored $RO_2$ isomerization and also contained seed aerosol to test effects of heterogeneous chemistry,

whereas exp. 4 favored the $RO_2$ + $RO_2$ reactions. This had minor effects on the general evolution of gas-phase products, that is, only a small fraction of the accretion ONs would partition to the particle phase (Wu et al., 2021). Experiments took place in Gothenburg using the laminar-flow Go:PAM reactor (Tsiligiannis et al., 2019; Watne et al., 2018) to test for a possible formation of the target compound(s) $C_4H_7NO_5$ from $NO_3$ oxidation of methyl vinyl ketone (MVK) (Table S8 in Supporting Information S1) and to constrain the instrument's sensitivity to ONs (Lopez-Hilfiker et al., 2016) (Table S3 in Supporting Information S1). Here $NO_3$ was introduced following the decomposition of $N_2O_5$ added via a diffusion source (Sections S2 and S5 in Supporting Information S1).

The ambient concentration profiles of the target isoprene products $C_4H_7NO_5$ were characterized during six field campaigns. Two campaigns took place in Asia, in Changping (near Beijing) (Le Breton, Wang et al., 2018) and Hong Kong as part of a project on photochemical smog in China (Hallquist et al., 2016). Two additional sites were located in Europe, in Jülich, Germany, during the JULIAC campaign and in Gothenburg, Sweden. Finally, data from Alabama, in the south-eastern USA during the Southern Oxidant and Aerosol Study (SOAS) (Lee et al., 2016) and from the Amazon rainforest were used to illustrate the omnipresence of the $C_4H_7NO_5$ isomers (Section S3 in Supporting Information S1). The $C_4H_7NO_5$ signal has also been observed in the free troposphere as part of flight measurements over the south-eastern USA during the Southeast Nexus campaign. However, a detailed discussion on those flights will be presented elsewhere.

The University of Gothenburg CIMS (GU-CIMS) was used for most field and laboratory measurements. The measurements from the SOAS campaign used the University of Washington CIMS (UW-CIMS), while the Amazon rainforest measurements used the University of Manchester CIMS (UMan-CIMS). Additional information on operational characteristics of CIMS during each campaign are given in Table S6 in Supporting Information S1. A bulk ON sensitivity factor of 4.8 ncps $ppt^{-1}$, derived during the SAPHIR experiment was used to convert the measured ONs signal to concentrations by GU-CIMS, where potential variability between ON was investigated using a voltage scanning method (see Section S2 in Supporting Information S1). UW-CIMS used a weighted isomer distribution of the isoprene-derived ON ($C_5H_9NO_4$, IHN) and UMan-CIMS used the isoprene-derived IEPOX as a proxy calibrant. More details on calibrations, sensitivity estimations and assumptions can be found in the SI (Section S2 & S3 in Supporting Information S1).

## 3. Results and Discussions

### 3.1. Experiments in the Atmospheric Simulation Chamber SAPHIR

During the experiments in the SAPHIR chamber, 24 mononitrates, 22 dinitrates and 18 accretion products were identified using the CIMS. Mononitrates dominated the spectrum ranging from 80.7% to 96.4% of the measured ONs, followed by dinitrates (3.3%–17.9%) and accretion products (0.2%–1.5%). Formation of ions assigned to the chemical composition $C_4H_7NO_5$ (Figure S2 in Supporting Information S1) were evident in all experiments. $C_4H_7NO_5$ signal was identified by the CIMS as an important nitrated product(s) together with the primary products $C_5H_9NO_5$ (hydroperoxide nitrates, INP), $C_5H_7NO_4$ (carbonyl nitrates, ICN), and $C_5H_9NO_4$ (hydroxy nitrates, IHN). Herein INP forms from $RO_2$ + $HO_2$ reaction whilst ICN and IHN largely form from $RO_2$ + $RO_2$ reaction.

Figure 1 depicts the time evolution of $C_4H_7NO_5$ (black), and the three other major primary oxidation products, $C_5H_9NO_5$ (blue), $C_5H_7NO_4$ (purple), and $C_5H_9NO_4$ (cyan), during the four selected experiments (Table S1 in Supporting Information S1). The relative contribution (red) of $C_4H_7NO_5$, expressed as the ratio of $C_4H_7NO_5$ over the total measured ONs signals by CIMS is also shown. The relative contribution is estimated assuming the same sensitivity for all the measured ONs. Generally, the time-series of the sum of measured mononitrates, dinitrates and accretion products followed the total gas-phase alkyl nitrates time evolution measured by a Thermal Dissociation Cavity Ring-down Spectrometer during the campaign (Brownwood et al., 2021), suggesting the CIMS total ONs signal includes the majority of the formed ON. In the dark the primary products increased rapidly after the injection of oxidant precursors and isoprene (Figure 1), especially $C_5H_9NO_5$ (INP), the dominant primary nighttime ON measured by the CIMS in all experiments. The $C_4H_7NO_5$ increased slowly and steadily, suggesting that there was no strong sink during the $NO_3$-dominated nighttime oxidation. This behavior would be typical for a closed shell product. However, the yield of $C_4H_7NO_5$ strongly depended on the chemical regime. In exp. 1 (Figure 1a) $RO_2$ + $HO_2$ reactions dominated (91%), while the $RO_2$ + $RO_2$ reactions were responsible for only a 4% loss (Brownwood et al., 2021). In exp. 2 (Figure 1b), the $RO_2$ + $RO_2$ reactions contributed up to 13% and the $RO_2$ + $HO_2$ reactions 53% of the loss rate of $RO_2$ (Brownwood et al., 2021). Under dominant $HO_2$ conditions

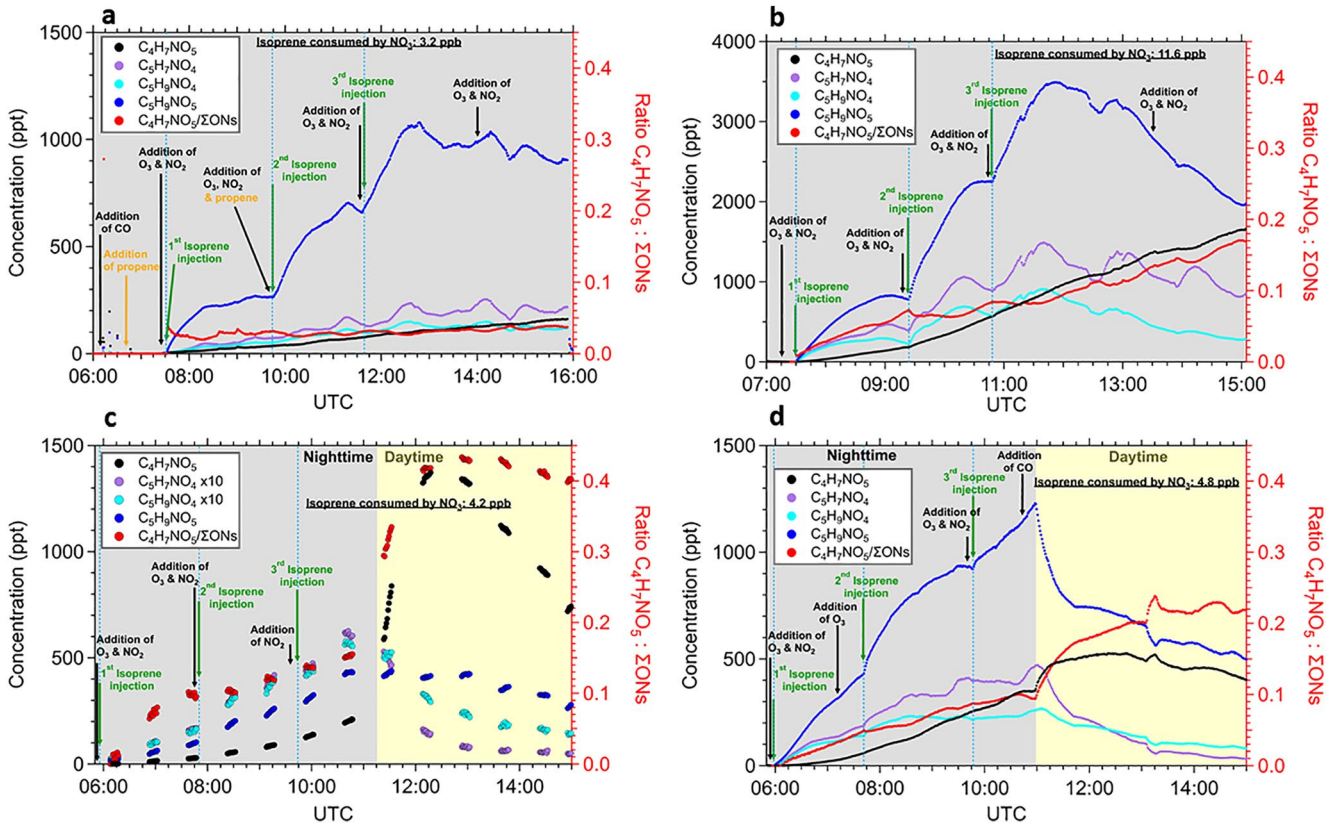


**Figure 1.** (a) Exp. 1 favoring $RO_2 + HO_2$ reactions. (b) Exp. 2 favoring $RO_2 + RO_2$ reactions. (c) Exp. 3 Nighttime-daytime transition focusing on the effect of the OH oxidation during daytime. (d) Exp. 4 Nighttime-daytime transition focusing on photolysis, using CO scavenger to suppress OH chemistry.

(exp. 1) the $C_4H_7NO_5$ formation was lower, and its relative contribution was always less than 5%, while the $C_5H_9NO_5$ (INP) contribution to ONs ranged between 21% and 33% due to the enhanced importance of the $HO_2$ reaction for the primary peroxy radical from isoprene + $NO_3$ reaction. When the $RO_2 + RO_2$ reactions were more important (exp. 2), the relative contribution of $C_4H_7NO_5$ increased, ultimately reaching over 15% and becoming the second major remaining product with a contribution close to that of $C_5H_9NO_5$.

Toward the end of exp. 1 and 2, when all isoprene was consumed, oxidant precursors were added without additional isoprene to enhance the oxidation of the products. For the experiment favoring $RO_2 + HO_2$ (exp. 1), this addition did not have a substantial effect on the products, including $C_4H_7NO_5$. For the conditions where $RO_2 + RO_2$ became more important (exp. 2), the signal of major primary products decreases, thus the relative contribution of $C_4H_7NO_5$ to the total ONs further increases from around 10% before the enhanced $NO_3$ oxidation to more than 15% at the end of the experiment. Thus, the $RO_2 + RO_2$ regime enables a subsequent acceleration of secondary chemistry and multi-generation products (Wu et al., 2021).

Nighttime to daytime transitions were included in exp. 3 and 4 by exposing the reaction mixture to sunlight by opening the roof of SAPHIR after a period of dark $NO_3$ oxidation (Figures 1c and 1d). The period of $NO_3$ oxidation was similar to exp. 2 without the last oxidant-only addition. The relative contribution of $C_4H_7NO_5$ to the total ONs was around 10% at the end of the nighttime period. Under daytime conditions in exp. 3, the ONs concentrations are expected to decrease under low NO conditions, as the carbonyl nitrates from isoprene react with OH radicals or are rapidly photolyzed (Müller et al., 2014; Xiong et al., 2016). This was also observed here for most of the ONs, for example, $C_5H_7NO_4$ (ICN) and $C_5H_9NO_4$ (IHN). However, the signal of the major product $C_5H_9NO_5$ did not decrease, that is, either $C_5H_9NO_5$ is not affected by daytime chemistry, or there are processes counteracting the loss, for example, formation of a nitrooxy hydroxyepoxide (INHE) by OH oxidation as described by Schwantes et al. (2015). The most pronounced change was the strong increase of the $C_4H_7NO_5$ signal, which became the dominant nitrated product(s), increasing from 10% at the end of nighttime to over 40% after an hour

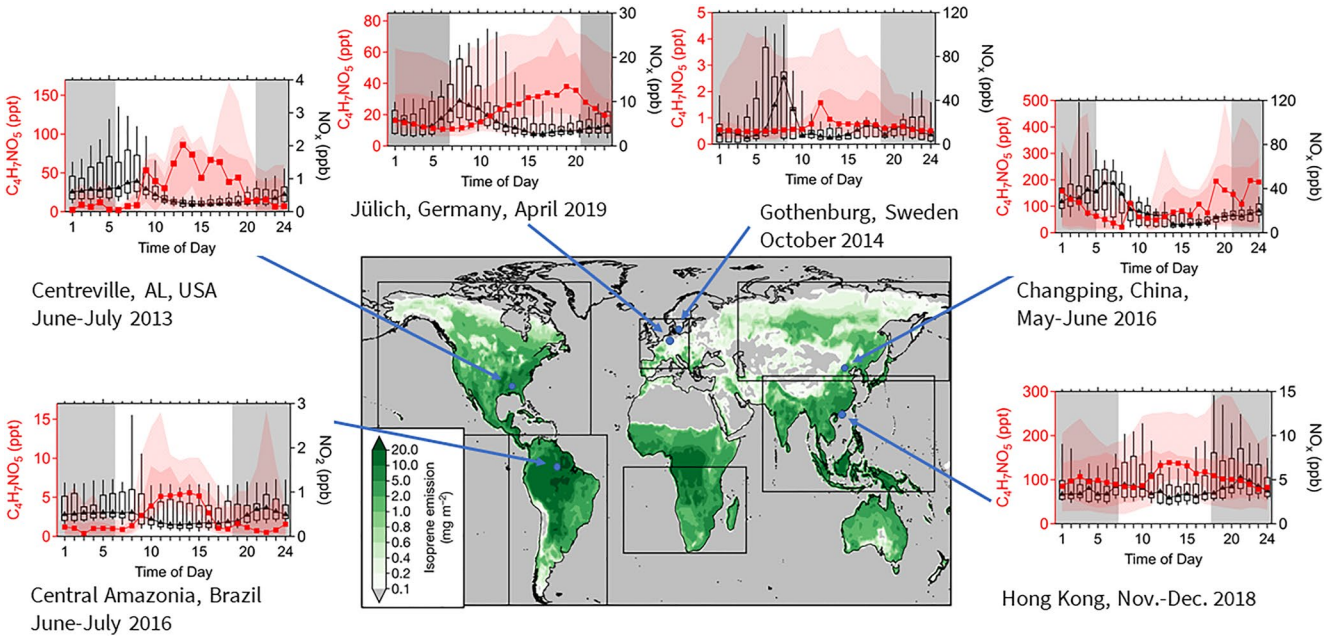


**Figure 2.** Median diurnal profile of the $C_4H_7NO_5$ and $NO_x$ in six different locations, with the 10th, 25th, 75th and 90th percentile. The gray areas in the plot indicate the nighttime period. Only the nitrogen dioxide profile is depicted in Amazonia. The map with the isoprene emissions is adapted from McFiggans et al. (2019).

of sunlight. At the onset of this enhanced increase of $C_4H_7NO_5$, there was no isoprene left in the chamber, clearly demonstrating the multi-generational sources of this product(s). In accordance with Schwantes et al. (2015) and Wennberg et al. (2018) we propose that all three major primary $C_5$ ONs ($C_5H_9NO_5$ (INP), $C_5H_7NO_4$ (ICN), and $C_5H_9NO_4$ (IHN)) can react with OH to form products with the chemical formula $C_4H_7NO_5$. After one and a half hours, $C_4H_7NO_5$ started decreasing due to chamber dilution, decreased availability of its precursors and slow but persistent removal processes, such as reaction with OH, photolysis.

To separately study the effect of photolysis, CO was added as an OH scavenger during the daytime period in exp. 4 (Figure 1d). In contrast to exp. 3, $C_5H_9NO_5$ decreased extremely rapidly as soon as the roof was opened. This difference to the daytime period of exp. 3 supports the existence of a formation pathway of $C_5H_9NO_5$ by OH oxidation that can balance out the significant loss by photolysis, as observed in exp. 4. In contrast, the $C_4H_7NO_5$ signal still increased in exp. 4 but to a lesser extent than in exp. 3. From the experiments in the simulation chamber, we conclude that formation pathways of $C_4H_7NO_5$ compound(s) exist in the dark (5%–17% of measured ONs), while during the following daytime, OH oxidation of multi-generational $NO_3$ products, together with a smaller contribution by photolysis, leads to a significant formation of $C_4H_7NO_5$, ultimately contributing more than 40% of measured ONs.

### 3.2. Ambient Measurements

$C_4H_7NO_5$ and the other major ONs observed in the chamber experiments were measured in six different field locations around the world. Overall, $C_4H_7NO_5$ signal was the dominant isoprene-derived nitrate measured during both daytime and nighttime at all the sampling sites (Figure S4 in Supporting Information S1). The ratio of $C_4H_7NO_5$ to the major primary $C_5$ ONs ($C_5H_9NO_5$, $C_5H_7NO_4$, and $C_5H_9NO_4$) often exhibited values above one throughout the day. However, the diurnal profile of $C_4H_7NO_5$ differed from site to site (Figure 2).

In Hong Kong – an isoprene-rich area with influence from anthropogenic emissions (Peng et al., 2022) – there were two peaks, one during daytime and one during nighttime. The nighttime peak becomes more prevalent if the period with high ONs formation is selected (between 14–25 November, Figure S5 in Supporting Information S1). Then, the median maximum value of the nighttime peak increases from 107 to 135 ppt and the daytime from 139 to 159 ppt. The fraction of $C_4H_7NO_5$ in the total measured isoprene-derived ONs ranged from 5% to 40% during the Hong Kong campaign (Figure S5 in Supporting Information S1).

The profile in Changping (near Beijing, China) showed a higher contribution during night than during day in conjunction with higher variability compared to Hong Kong. The isoprene mean diurnal profile had a peak at 14:00 and the isoprene concentrations were almost always above zero, even during nighttime (Le Breton, Hallquist et al., 2018). The local meteorology has a pronounced impact on the type of air masses reaching Beijing, for example, the wind speed has high values during the day and low values during the night (Le Breton, Wang et al., 2018).

The two locations in Europe are characterized by low regional isoprene emissions, especially Gothenburg, Sweden, and as expected the $C_4H_7NO_5$ signal was much lower compared to the other sites. In Gothenburg, $C_4H_7NO_5$ had a weak peak around noon, whilst there was a clear wide peak in the early evening in Jülich, Germany.

The Southeastern USA represents an area with high isoprene concentrations and low to modest $NO_x$ emissions outside of urban areas. Centreville is a rural site with low average $NO_x$ concentrations (Edwards et al., 2017; Lee et al., 2016). There, $C_4H_7NO_5$ had a diurnal profile with a clear peak during daytime with high variability. The strong increase during morning (8:00–10:00, local time) was likely due to sampling of the residual layer after the morning breakup of the nocturnal boundary layer, enabling both production and downward transport to contribute to increasing $C_4H_7NO_5$.

Finally, the Amazon rainforest measurements showed a strong daytime peak. The site is remote from human sources, exhibiting very low $NO_x$ concentrations (average = 0.62 ppb), and consequently lower $C_4H_7NO_5$ compared to the other isoprene-rich areas, Hong Kong with much higher $NO_x$ (average = 5 ppb) and southeastern USA with slightly higher $NO_x$ levels (average = 0.67 ppb). The corresponding ozone concentrations at the measurement sites are given in SI (Table S5 in Supporting Information S1).

The correlations of $C_4H_7NO_5$ with the other major primary isoprene-derived ONs ($C_5H_9NO_5$, $C_5H_7NO_4$, and $C_5H_9NO_4$) varied at the different sites (Table S4 in Supporting Information S1). The isoprene concentration, the origin and chemical age of the air masses, and meteorology all influenced the correlation slope and the correlation coefficient $R^2$. For example, in Gothenburg local isoprene emissions are low and the correlation was likely driven by variability in air mass origin, with primary and multi-generational isoprene products like $C_4H_7NO_5$ exhibiting high correlation. In contrast, in areas with high isoprene emissions, such as the Amazon rainforest, the correlation between first and multi-generational products was significantly weaker, illustrating the influence of air mass aging and the expected sequential production from isoprene.

Based on the chamber experiments, $C_4H_7NO_5$ was the most abundant isoprene-derived ON measured by the CIMS during daytime, but not during nighttime. The ambient measurements also showed $C_4H_7NO_5$ was the dominant isoprene-derived ON during daytime. However, at the ambient measurements $C_4H_7NO_5$ was also the highest isoprene-derived measured ON signal during nighttime. The dominant role for $C_4H_7NO_5$ observed during nighttime could be due to efficient accumulation. Under daytime ambient conditions $C_4H_7NO_5$ can be also produced in relatively high amounts via OH oxidation of other isoprene-nitrated products ($C_5H_9NO_5$ (INP), $C_5H_7NO_4$ (ICN), and $C_5H_9NO_4$ (IHN)). The chamber experiments showed that $C_4H_7NO_5$ did not have any major losses by $NO_3$ and $O_3$. $C_4H_7NO_5$ was also not affected drastically by the additions of isoprene or extra non-OH oxidant during the experiments. The lack of a carbon-carbon double bond gives $C_4H_7NO_5$ a low reactivity toward the $NO_3$ and $O_3$ oxidants dominant during the night. This produces longer residence times than other major ONs that enhance accumulation of the produced $C_4H_7NO_5$.

### 3.3. Formation and Accumulation of $C_4$ Compounds

A key feature from the experiments in the chamber was the pronounced increase in concentration of $C_4H_7NO_5$ during transitions from night to day conditions. At some of the ambient sites there was also such a tendency, but it was often concealed by the overwhelming contribution of the daytime oxidation of freshly emitted isoprene, especially for the sites with large isoprene emissions (Amazon rainforest, SE-USA, and Hong Kong). A major result from our work is the demonstration that $C_4H_7NO_5$ isomers are multi-generational products of several $C_5$ compounds. In the nighttime-daytime transition this was evident both with and without OH radical chemistry (Figures 1c and 1d).

During daytime oxidation, $C_4H_7NO_5$ isomers are expected to form by OH-initiated oxidation via a number of pathways. For example, two major unsaturated products from OH-initiated isoprene oxidation are MVK and

methacrolein (MACR). OH addition to these compounds, followed by $O_2$ addition to form a peroxy radical and subsequent NO reaction to alkoxy radicals, leads to the formation of nitrooxy ketones and nitrooxy aldehydes, with the chemical formula $C_4H_7NO_5$ (Jenkin et al., 2015; Praske et al., 2015). OH oxidation of $C_5$ ONs ($C_5H_9NO_5$ (INP), $C_5H_7NO_4$ (ICN), and $C_5H_9NO_4$ (IHN)) can also lead to $C_4H_7NO_5$ compounds (Schwantes et al., 2015; Wennberg et al., 2018). The initial peroxy radicals from the aforementioned $C_5$ ONs also form alkoxy radicals from reaction with NO, or $HO_2$ where a fraction can decompose to $C_4H_7NO_5$ isomers (Novelli et al., 2021; Vereecken & Peeters, 2009; Wennberg et al., 2018).

In contrast to the daytime formation of $C_4H_7NO_5$, where several pathways from different precursors have been suggested, little is known about nighttime formation. The most plausible reactions forming a $C_4H_7NO_5$ isomer are listed in the supplemental and are summarized here.

$$\mathrm{MVK} + \mathrm{NO_3} \rightarrow \cdots \rightarrow C_4H_7NO_5\ (\mathrm{ketone}) \tag{R1}$$

$$\mathrm{MACR} + \mathrm{NO_3} \rightarrow \cdots \rightarrow C_4H_7NO_5\ (\mathrm{aldehyde}) \tag{R2}$$

$$4,1-\mathrm{IHN}\ (C_5H_9NO_4) + \mathrm{NO_3} \rightarrow \cdots \rightarrow C_4H_7NO_5\ (\mathrm{ketone}) \tag{R3}$$

$$1,2-\mathrm{IHN}\ (C_5H_9NO_4) + \mathrm{NO_3} \rightarrow \cdots \rightarrow C_4H_7NO_5\ (\mathrm{aldehyde}) \tag{R4}$$

$$4,3-\mathrm{IHN}\ (C_5H_9NO_4) + \mathrm{NO_3} \rightarrow \cdots \rightarrow C_4H_7NO_5\ (\mathrm{ketone}) \tag{R5}$$

$$\mathrm{HC4CCHO}\ (C_5H_8O_2) + \mathrm{NO_3} \rightarrow \cdots \rightarrow C_4H_7NO_5\ (\mathrm{ketone}) \tag{R6}$$

$$\mathrm{HC4ACHO}\ (C_5H_8O_2) + \mathrm{NO_3} \rightarrow \cdots \rightarrow C_4H_7NO_5\ (\mathrm{aldehyde}) \tag{R7}$$

$$4,1-\mathrm{ICN-RO_2}\ (C_5H_8NO_7) \rightarrow \cdots \xrightarrow{\text{Decomposition}} C_4H_7NO_5\ (\mathrm{aldehyde}) \tag{R8}$$

$$1,4-\mathrm{ICN-RO_2}\ (C_5H_8NO_7) \rightarrow \cdots \xrightarrow{\text{Decomposition}} C_4H_7NO_5\ (\mathrm{ketone}) \tag{R9}$$

$$\mathrm{Nitrated\ peroxy\ acids} \rightarrow \cdots \xrightarrow{\text{Decomposition}} C_4H_7NO_5 \tag{R10}$$

$$\mathrm{Nitrated\ epoxides} \rightarrow \cdots \xrightarrow{\text{Decomposition}} C_4H_7NO_5 \tag{R11}$$

Although MVK and MACR oxidation by $NO_3$ radicals is slow (Kwok et al., 1996) these major products could provide a persistent source of $C_4H_7NO_5$ (Reactions R1 and R2). To verify this, further experiments were performed in an oxidation flow reactor, the Go:PAM (Table S8 in Supporting Information S1) showing a direct source of $C_4H_7NO_5$ from $NO_3$-initiated MVK oxidation (Figure S10 in Supporting Information S1). However, the estimated maximum contribution from this pathway is very low and cannot explain the observed formation in the SAPHIR chamber.

Formation of $C_4H_7NO_5$ during nighttime may also be due to the $NO_3$-initiated oxidation of first-generation hydroxy nitrate isomers (IHN, $C_5H_9NO_4$) (Reactions R3, R4 and R5). Here $C_4H_7NO_5$ isomers are formed via decomposition of produced alkoxy radicals, with the specific pathway depending on the isomer. The structural differences of the IHN-isomers also affect their rate constants with $NO_3$ radicals, spanning an order of magnitude (Pfrang et al., 2006; Wennberg et al., 2018). These pathways release $NO_2$ back to the system, but such an increase of $NO_2$ was not observed in the SAPHIR chamber experiments. Also, structure-activity relationship (SAR) estimates that the decomposition channel is not dominant (Novelli et al., 2021). Thus, these reactions are likely insignificant.

Another potential pathway is the further oxidation of hydroxy carbonyls (HC4CCHO and HC4ACHO, $C_5H_8O_2$) by $NO_3$ (Reactions R6 and R7). The peroxy radicals formed from oxidation of $C_5H_8O_2$ can undergo isomerization and decomposition leading to the formation of a $C_4H_7NO_5$ nitrooxy ketone or nitrooxy aldehyde (Figure S6 in Supporting Information S1) (Wu et al., 2021). The peroxy radicals $C_5H_8NO_7$ can also form a $C_4H_7NO_5$ nitrooxy carbonyl by decomposing (Reactions R8 and R9) (Wennberg et al., 2018). Those parent peroxy radicals ($C_5H_8NO_7$) can be formed either by further autoxidation of the initial peroxy radical formed by $NO_3$ oxidation (i.e., isomerization and $O_2$ addition) or by OH-initiated oxidation of $C_5H_7NO_4$ isomers. Finally, peroxy acids and epoxides formed by the $NO_3$-initiated oxidation of isoprene (Vereecken et al., 2021) may decompose

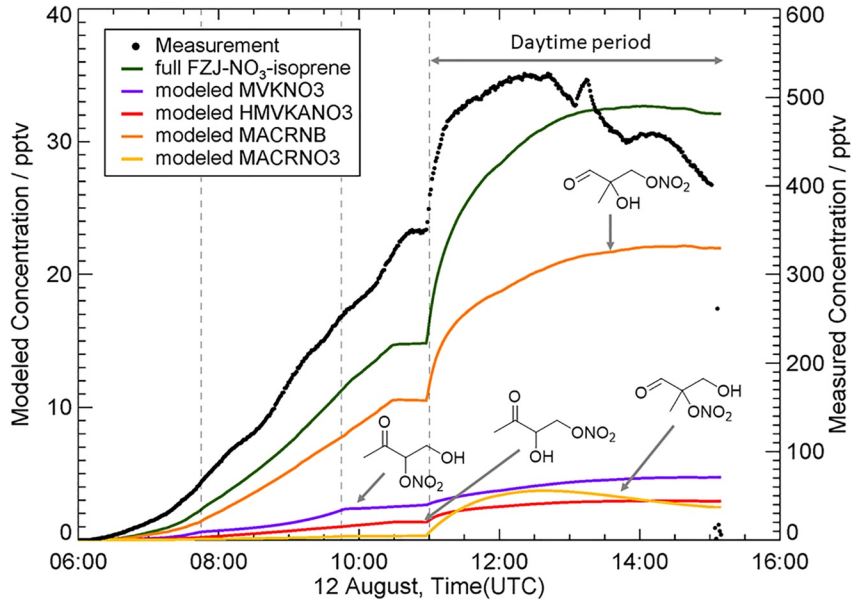


**Figure 3.** Comparison of the measured (black) and modeled (green) $C_4H_7NO_5$ formation during exp. 4 (nighttime to daytime transition using an OH scavenger). The "full FZJ-$NO_3$-isoprene" sum of the four main isomers is compared against the I-CIMS measurements.

forming $C_4H_7NO_5$ isomers (Reactions R10 and R11). However, this chemistry is not well-known and needs further attention.

To test potential contributions of the suggested pathways, the FZJ-$NO_3$-Isoprene mechanism presented by Vereecken et al. (2021), which in turn is based on the MCMv3.3.1 (Jenkin et al., 1997; Jenkin et al., 2015; Saunders et al., 2003) and on the more explicit descriptions from the CalTech mechanism (Wennberg et al., 2018) was expanded by the additional pathways as described above and summarized in the SI (Section S4 in Supporting Information S1). The model considered Reactions R6–R9. Figure 3 shows the calculated trends of four selected isomers (i.e., MACRNB, MVKNO3, HMVKANO3 and MACRNO3, with the corresponding structures shown, see also Table S7 in Supporting Information S1) for the nighttime to daytime transition experiment in the SAPHIR chamber (exp. 4, Figure 1d) with OH scavenger, where only photolysis was important. The model predicts that the dominant $C_4H_7NO_5$ nitrooxy isomer under nighttime conditions should be the aldehyde MACRNB followed by MVKNO3, HMVKANO3 and MACRNO3 in lower concentrations (Figure 3). The overall trend of the model matches the behavior of the measurements. However, there remains a significant discrepancy in the absolute concentrations (see Section S4, Figures S7–S9 in Supporting Information S1). It is not clear why there is a such large discrepancy and as outlined in the SI some measurement concerns are addressed. Still, the general measurement agreements with for example, the total alkyl nitrates (Brownwood et al., 2021) and Br-CIMS measurements (Section S2 in Supporting Information S1) clearly illustrate that the $C_4H_7NO_5$ isomers are important products. This discrepancy could be due to unknown formation pathways for example, secondary formation of $C_4H_7NO_5$ isomers from decomposition of epoxides and peroxides, highlighted as major contributing species in the model. It is not clear if produced epoxides and peroxides are unstable and can decompose into $C_4$ products ($C_4H_7NO_5$ being one of them) in the gas phase or on available surfaces, thus explaining why only low concentration of these were observed. Finally, the possibility of some production by OH oxidation under dark conditions cannot be ruled out, but certainly the contribution was small as isoprene loss due to $NO_3$ was calculated to be around 90% (Brownwood et al., 2021) and the impact of isoprene + OH on the total yield of $C_4H_7NO_5$ was below 5% for all modeled experiments (more details in Section S1 in Supporting Information S1). However, further exploration and evaluation of these pathways are beyond the scope of this work.

In the model, the increase of $C_4H_7NO_5$ under the OH scavenged/photolytic conditions is due to the formation of the nitrooxy aldehydes MACRNO3 and MACRNB. The photolysis of two hydroperoxy aldehydes (HPALD, with chemical formula $C_5H_8O_3$), formed via isomerization of isoprene hydroxy peroxy radicals, can lead to $C_4H_7NO_5$ after a subsequent $NO_2$ addition (Wennberg et al., 2018). One isomer forms the nitrooxy aldehyde MACRNO3

while the other forms the nitrooxy ketone MVKNO3. However, these pathways do not represent the major loss of HPALDs (Wennberg et al., 2018). Xiong et al. (2016) have suggested that $C_5H_7NO_4$ (ICN) can dissociate via photolysis and then react with $O_2$ and $HO_2$ to form a vinyl hydroperoxide with chemical formula $C_4H_7NO_5$. Since no mechanistic description was given, in this work the photolysis was implemented as given in Wennberg et al. (2018). Müller et al. (2014) have suggested that photolysis is the dominant sink of the isoprene-derived carbonyl nitrates such as MACRNO3, MVKNO3 and HMVKANO3 under atmospheric relevant conditions, but in the model, rapid formation from HPALD and other sources counteracts their loss, leading to constant or increasing concentrations.

In addition to photolysis, the residual nighttime primary products can also react with OH radicals during daytime. We attribute the rapid $C_4H_7NO_5$ formation in exp. 3 (Figure 1c) to the OH-initiated oxidation of the three other major ONs ($C_5H_9NO_5$, $C_5H_7NO_4$, and $C_5H_9NO_4$), which has also been proposed in previous studies (Wennberg et al., 2018) (Section S4 in Supporting Information S1). The efficiency of these pathways in forming $C_4H_7NO_5$ must be high in order to fully explain the observations in both the findings in the SAPHIR chamber and the field observations.

## 4. Atmospheric Implication and Conclusion

The $C_4H_7NO_5$ isomers are important products of isoprene oxidation in $NO_x$-influenced regions. Ambient measurements showed that $C_4H_7NO_5$ compound(s) typically have higher concentrations than the other three major ONs ($C_5H_9NO_5$ (INP), $C_5H_7NO_4$ (ICN), and $C_5H_9NO_4$ (IHN)) during both night and day. For nighttime conditions this finding appears in contradiction to our chamber measurements, where $C_4H_7NO_5$ was only dominant during daytime. We found that $C_4H_7NO_5$ isomers are multi-generation products, with no remaining C=C bonds, in the isoprene degradation mechanism, formed from both OH and $NO_3$-radical initiated oxidation where observations in ambient air can be expected from air mass aging processes.

$C_4H_7NO_5$ nighttime production was investigated here in detail. We suggest that the decomposition of the $C_5H_8NO_7$ peroxy radicals from $NO_3$-initiated chemistry, the oxidation of hydroxy carbonyls (HC4CCHO and HC4ACHO) ($C_5H_8O_2$) by $NO_3$ and the decomposition of nitrated epoxides and peroxides are mainly responsible for nighttime production. The relative contribution of $C_4H_7NO_5$ to total measured ONs increased in chamber experiments when $RO_2$ loss was enhanced by $RO_2$ + $RO_2$ reactions. Furthermore, the chamber experiments showed that $C_4H_7NO_5$ formation was lower during nighttime when $RO_2$ + $HO_2$ reactions were dominant. According to model calculations, the isomers MACRNB and MVKNO3 have the highest contribution to $C_4H_7NO_5$ formation under dark conditions. Although most of the other ONs, generated initially in higher yields, react away after transition into the daytime, $C_4H_7NO_5$ concentration increased, indicating a slower reactivity together with continuing or enhanced production.

The lack of a carbon-carbon double bond lowers its reactivity and thus increases its lifetime. Slow oxidation and photolytic reactions of $C_4H_7NO_5$ lead to longer lifetimes than those of the $C_5$ ONs formed in higher yields from isoprene. This can explain the higher effective concentrations of $C_4H_7NO_5$ in the residual boundary layer and dominance in various ambient conditions. This suggests that $C_4H_7NO_5$ isoprene ONs could be important as a long-term organic reservoir species of $NO_x$, in comparison to the other more reactive isoprene-derived ONs. The importance of further understanding the properties of the different isomers is highlighted by a recent study (Vasquez et al., 2020) which showed that the isoprene nitrate isomer 1,2-IHN can efficiently remove $NO_x$ from the atmosphere, whereas other isomers cannot. To further understand the distribution of isomers and their specific chemistry, further studies are needed using a broader range of methods. Especially a focus on the predicted dominant product family of the nitrated epoxides (Vereecken et al., 2021), whose secondary chemistry and therefore potential for forming $C_4H_7NO_5$ is largely unknown, is a necessity. Finally, the isoprene-derived ONs, of which $C_4H_7NO_5$ is a dominant species, can thus be important for the formation of ozone, with ONs formed during nighttime affecting the initiation of tropospheric ozone formation during the following day.

## Conflict of Interest

The authors declare no conflicts of interest relevant to this study.

## Data Availability Statement

The data used in this study are permanently archived at https://doi.org/10.5878/wfv9-a491.

**Acknowledgments**
The authors acknowledge SAPHIR team of the Institute for Energy and Climate (IEK-8), Forschungszentrum Jülich for their support and technical help during the isoprene + $NO_3$ experiments at the SAPHIR chamber, the team of the NO3Isop, JULIAC, Hong Kong, Changping, Amazon, SOAS and Gothenburg campaigns. This research has been supported by the European Research Council (ERC) (SARLEP grant agreement no. 681529), European Commission (EC) under the European Union's Horizon 2020 research and innovation program (Eurochamp 2020 grant agreement no. 730997 and FORCeS grant agreement no. 821205), Vetenskapsrådet (VR, Grant Nos. 2014–05332 and 2018–04430), and Svenska Forskningsrådet Formas (Grant Nos. 2015–1537 and 2019–586). A. Mayhew acknowledges the Natural Environment Research Council for a PhD studentship as part of the PANORAMA DTP. T. Wang is supported by the Hong Kong Research Grants Council (project no. A-PolyU502/16), and he thanks the Hong Kong Environmental Protection for providing access to its air monitoring site. The Amazon deployment was supported by the FAPESP-University of Manchester SPRINT initiative.

## References

Brownwood, B., Turdziladze, A., Hohaus, T., Wu, R., Mentel, T. F., Carlsson, P. T. M., et al. (2021). Gas-particle partitioning and SOA yields of organonitrate products from $NO_3$-initiated oxidation of isoprene under varied chemical regimes. *ACS Earth and Space Chemistry*, *5*(4), 785–800. https://doi.org/10.1021/acsearthspacechem.0c00311

Bryant, D. J., Dixon, W. J., Hopkins, J. R., Dunmore, R. E., Pereira, K. L., Shaw, M., et al. (2020). Strong anthropogenic control of secondary organic aerosol formation from isoprene in Beijing. *Atmospheric Chemistry and Physics*, *20*(12), 7531–7552. https://doi.org/10.5194/acp-20-7531-2020

D'Ambro, E. L., Lee, B. H., Liu, J., Shilling, J. E., Gaston, C. J., Lopez-Hilfiker, F. D., et al. (2017). Molecular composition and volatility of isoprene photochemical oxidation secondary organic aerosol under low- and high-NOx conditions. *Atmospheric Chemistry and Physics*, *17*(1), 159–174. https://doi.org/10.5194/acp-17-159-2017

Dewald, P., Liebmann, J. M., Friedrich, N., Shenolikar, J., Schuladen, J., Rohrer, F., et al. (2020). Evolution of $NO_3$ reactivity during the oxidation of isoprene. *Atmospheric Chemistry and Physics*, *20*(17), 10459–10475. https://doi.org/10.5194/acp-20-10459-2020

Edwards, P. M., Aikin, K. C., Dube, W. P., Fry, J. L., Gilman, J. B., de Gouw, J. A., et al. (2017). Transition from high- to low-NOx control of night-time oxidation in the southeastern US. *Nature Geoscience*, *10*(7), 490–495. https://doi.org/10.1038/ngeo2976

Fry, J. L., Brown, S. S., Middlebrook, A. M., Edwards, P. M., Campuzano-Jost, P., Day, D. A., et al. (2018). Secondary organic aerosol (SOA) yields from $NO_3$ radical + isoprene based on nighttime aircraft power plant plume transects. *Atmospheric Chemistry and Physics*, *18*(16), 11663–11682. https://doi.org/10.5194/acp-18-11663-2018

Fuchs, H., Novelli, A., Rolletter, M., Hofzumahaus, A., Pfannerstill, E. Y., Kessel, S., et al. (2017). Comparison of OH reactivity measurements in the atmospheric simulation chamber SAPHIR. *Atmospheric Measurement Techniques*, *10*, 4023–4053. https://doi.org/10.5194/amt-10-4023-2017

Glasius, M., & Goldstein, A. H. (2016). Recent discoveries and future challenges in atmospheric organic chemistry. *Environmental Science and Technology*, *50*(6), 2754–2764. https://doi.org/10.1021/acs.est.5b05105

Guenther, A. B., Jiang, X., Heald, C. L., Sakulyanontvittaya, T., Duhl, T., Emmons, L. K., & Wang, X. (2012). The Model of Emissions of Gases and Aerosols from Nature version 2.1 (MEGAN2.1): An extended and updated framework for modeling biogenic emissions. *Geoscientific Model Development*, *5*(6), 1471–1492. https://doi.org/10.5194/gmd-5-1471-2012

Hallquist, M., Munthe, J., Hu, M., Wang, T., Chan, C. K., Gao, J., et al. (2016). Photochemical smog in China: Scientific challenges and implications for air-quality policies. *National Science Review*, *3*(4), 401–403. https://doi.org/10.1093/nsr/nww080

Hallquist, M., Wenger, J. C., Baltensperger, U., Rudich, Y., Simpson, D., Claeys, M., et al. (2009). The formation, properties and impact of secondary organic aerosol: Current and emerging issues. *Atmospheric Chemistry and Physics*, *9*(14), 5155–5236. https://doi.org/10.5194/acp-9-5155-2009

Hamilton, J. F., Bryant, D. J., Edwards, P. M., Ouyang, B., Bannan, T. J., Mehra, A., et al. (2021). Key role of $NO_3$ radicals in the production of isoprene nitrates and nitrooxyorganosulfates in beijing. *Environmental science and technology*, *55*, 842–853. https://doi.org/10.1021/acs.est.0c05689

Jenkin, M. E., Saunders, S. M., & Pilling, M. J. (1997). The tropospheric degradation of volatile organic compounds: A protocol for mechanism development. *Atmospheric Environment*, *31*, 81–104. https://doi.org/10.1016/S1352-2310(96)00105-7

Jenkin, M. E., Young, J. C., & Rickard, A. R. (2015). The MCM v3.3.1 degradation scheme for isoprene. *Atmospheric Chemistry and Physics*, *15*(20), 11433–11459. https://doi.org/10.5194/acp-15-11433-2015

Kenagy, H. S., Sparks, T. L., Wooldridge, P. J., Weinheimer, A. J., Ryerson, T. B., Blake, D. R., et al. (2020). Evidence of nighttime production of organic nitrates during SEAC4RS, frappé, and KORUS-AQ. *Geophysical Research Letters*, *47*(11), e2020GL087860. https://doi.org/10.1029/2020gl087860

Kiendler-Scharr, A., Mensah, A. A., Friese, E., Topping, D., Nemitz, E., Prevot, A. S. H., et al. (2016). Ubiquity of organic nitrates from nighttime chemistry in the European submicron aerosol. *Geophysical Research Letters*, *43*(14), 7735–7744. https://doi.org/10.1002/2016gl069239

Kleindienst, T. E., Lewandowski, M., Offenberg, J. H., Jaoui, M., & Edney, E. O. (2007). Ozone-isoprene reaction: Re-examination of the formation of secondary organic aerosol. *Geophysical Research Letters*, *34*(1), L01805. https://doi.org/10.1029/2006gl027485

Kroll, J. H., Ng, N. L., Murphy, S. M., Flagan, R. C., & Seinfeld, J. H. (2005). Secondary organic aerosol formation from isoprene photooxidation under high-NOx conditions. *Geophysical Research Letters*, *32*(18). https://doi.org/10.1029/2005gl023637

Kwan, A. J., Chan, A. W. H., Ng, N. L., Kjaergaard, H. G., Seinfeld, J. H., & Wennberg, P. O. (2012). Peroxy radical chemistry and OH radical production during the $NO_3$-initiated oxidation of isoprene. *Atmospheric Chemistry and Physics*, *12*(16), 7499–7515. https://doi.org/10.5194/acp-12-7499-2012

Kwok, E. S. C., Aschmann, S. M., Arey, J., & Atkinson, R. (1996). Product formation from the reaction of the $NO_3$ radical with isoprene and rate constants for the reactions of methacrolein and methyl vinyl ketone with the $NO_3$ radical. *International Journal of Chemical Kinetics*, *28*(12), 925–934. https://doi.org/10.1002/(sici)1097-4601(1996)28:12<925::Aid-kin10>3.0.Co;2-b

Le Breton, M., Hallquist, Å. M., Pathak, R. K., Simpson, D., Wang, Y., Johansson, J., et al. (2018). Chlorine oxidation of VOCs at a semi-rural site in beijing: Significant chlorine liberation from ClNO2 and subsequent gas- and particle-phase Cl–voc production. *Atmospheric Chemistry and Physics*, *18*(17), 13013–13030. https://doi.org/10.5194/acp-18-13013-2018

Le Breton, M., Wang, Y., Hallquist, Å. M., Pathak, R. K., Zheng, J., Yang, Y., et al. (2018). Online gas- and particle-phase measurements of organosulfates, organosulfonates and nitrooxy organosulfates in Beijing utilizing a FIGAERO ToF-CIMS. *Atmospheric Chemistry and Physics*, *18*(14), 10355–10371. https://doi.org/10.5194/acp-18-10355-2018

Lee, B. H., Lopez-Hilfiker, F. D., Mohr, C., Kurten, T., Worsnop, D. R., & Thornton, J. A. (2014). An iodide-adduct high-resolution time-of-flight chemical-ionization mass spectrometer: Application to atmospheric inorganic and organic compounds. *Environmental Science and Technology*, *48*(11), 6309–6317. https://doi.org/10.1021/es500362a

Lee, B. H., Mohr, C., Lopez-Hilfiker, F. D., Lutz, A., Hallquist, M., Lee, L., et al. (2016). Highly functionalized organic nitrates in the southeast United States: Contribution to secondary organic aerosol and reactive nitrogen budgets. *Proceedings of the National Academy of Sciences of the USA*, *113*(6), 1516–1521. https://doi.org/10.1073/pnas.1508108113

Lee, L., Teng, A. P., Wennberg, P. O., Crounse, J. D., & Cohen, R. C. (2014). On rates and mechanisms of OH and $O_3$ reactions with isoprene-derived hydroxy nitrates. *The Journal of Physical Chemistry A*, *118*(9), 1622–1637. https://doi.org/10.1021/jp4107603

Li, J., Wang, Y., & Qu, H. (2019). Dependence of summertime surface ozone on $NO_x$ and VOC emissions over the United States: Peak time and value. *Geophysical Research Letters*, *46*(6), 3540–3550. https://doi.org/10.1029/2018gl081823

Lopez-Hilfiker, F. D., Iyer, S., Mohr, C., Lee, B. H., D'Ambro, E. L., Kurtén, T., & Thornton, J. A. (2016). Constraining the sensitivity of iodide adduct chemical ionization mass spectrometry to multifunctional organic molecules using the collision limit and thermodynamic stability of iodide ion adducts. *Atmospheric Measurement Techniques*, *9*(4), 1505–1512. https://doi.org/10.5194/amt-9-1505-2016

McFiggans, G., Mentel, T. F., Wildt, J., Pullinen, I., Kang, S., Kleist, E., et al. (2019). Secondary organic aerosol reduced by mixture of atmospheric vapours. *Nature*, *565*(7741), 587–593. https://doi.org/10.1038/s41586-018-0871-y

Müller, J. F., Peeters, J., & Stavrakou, T. (2014). Fast photolysis of carbonyl nitrates from isoprene. *Atmospheric Chemistry and Physics*, *14*(5), 2497–2508. https://doi.org/10.5194/acp-14-2497-2014

Ng, N. L., Kwan, A. J., Surratt, J. D., Chan, A. W. H., Chhabra, P. S., Sorooshian, A., et al. (2008). Secondary organic aerosol (SOA) formation from reaction of isoprene with nitrate radicals ($NO_3$). *Atmospheric Chemistry and Physics*, *8*(14), 4117–4140. https://doi.org/10.5194/acp-8-4117-2008

Novelli, A., Cho, C., Fuchs, H., Hofzumahaus, A., Rohrer, F., Tillmann, R., et al. (2021). Experimental and theoretical study on the impact of a nitrate group on the chemistry of alkoxy radicals. *Physical Chemistry Chemical Physics*, *23*(9), 5474–5495. https://doi.org/10.1039/D0CP05555G

Novelli, A., Vereecken, L., Bohn, B., Dorn, H. P., Gkatzelis, G. I., Hofzumahaus, A., et al. (2020). Importance of isomerization reactions for OH radical regeneration from the photo-oxidation of isoprene investigated in the atmospheric simulation chamber SAPHIR. *Atmospheric Chemistry and Physics*, *20*(6), 3333–3355. https://doi.org/10.5194/acp-20-3333-2020

Peeters, J., Müller, J.-F., Stavrakou, T., & Nguyen, V. S. (2014). Hydroxyl radical recycling in isoprene oxidation driven by hydrogen bonding and hydrogen tunneling: The upgraded LIM1 mechanism. *The Journal of Physical Chemistry A*, *118*(38), 8625–8643. https://doi.org/10.1021/jp5033146

Peng, X., Wang, T., Wang, W., Ravishankara, A. R., George, C., Xia, M., et al. (2022). Photodissociation of particulate nitrate as a source of daytime tropospheric Cl2. *Nature Communications*, *13*, 939. https://doi.org/10.1038/s41467-022-28383-9

Pfrang, C., King, M. D., Canosa-Mas, C. E., & Wayne, R. P. (2006). Structure–activity relations (SARs) for gas-phase reactions of $NO_3$, OH and $O_3$ with alkenes: An update. *Atmospheric Environment*, *40*(6), 1180–1186. https://doi.org/10.1016/j.atmosenv.2005.09.080

Praske, E., Crounse, J. D., Bates, K. H., Kurtén, T., Kjaergaard, H. G., & Wennberg, P. O. (2015). Atmospheric fate of methyl vinyl ketone: Peroxy radical reactions with NO and $HO_2$. *The Journal of Physical Chemistry A*, *119*(19), 4562–4572. https://doi.org/10.1021/jp5107058

Rohrer, F., Bohn, B., Brauers, T., Brüning, D., Johnen, F. J., Wahner, A., & Kleffmann, J. (2005). Characterisation of the photolytic HONO-source in the atmosphere simulation chamber SAPHIR. *Atmospheric Chemistry and Physics*, *5*(8), 2189–2201. https://doi.org/10.5194/acp-5-2189-2005

Saunders, S. M., Jenkin, M. E., Derwent, R. G., & Pilling, M. J. (2003). Protocol for the development of the Master Chemical Mechanism, MCM v3 (Part A): Tropospheric degradation of non-aromatic volatile organic compounds. *Atmospheric Chemistry and Physics*, *3*, 161–180. https://doi.org/10.5194/acp-3-161-2003

Schwantes, R. H., Charan, S. M., Bates, K. H., Huang, Y., Nguyen, T. B., Mai, H., et al. (2019). Low-volatility compounds contribute significantly to isoprene secondary organic aerosol (SOA) under high-NOx conditions. *Atmospheric Chemistry and Physics*, *19*(11), 7255–7278. https://doi.org/10.5194/acp-19-7255-2019

Schwantes, R. H., Emmons, L. K., Orlando, J. J., Barth, M. C., Tyndall, G. S., Hall, S. R., et al. (2020). Comprehensive isoprene and terpene gas-phase chemistry improves simulated surface ozone in the southeastern US. *Atmospheric Chemistry and Physics*, *20*(6), 3739–3776. https://doi.org/10.5194/acp-20-3739-2020

Schwantes, R. H., Teng, A. P., Nguyen, T. B., Coggon, M. M., Crounse, J. D., St Clair, J. M., et al. (2015). Isoprene $NO_3$ oxidation products from the $RO_2 + HO_2$ pathway. *The Journal of Physical Chemistry A*, *119*(40), 10158–10171. https://doi.org/10.1021/acs.jpca.5b06355

Shrivastava, M., Cappa, C. D., Fan, J., Goldstein, A. H., Guenther, A. B., Jimenez, J. L., et al. (2017). Recent advances in understanding secondary organic aerosol: Implications for global climate forcing. *Reviews of Geophysics*, *55*(2), 509–559. https://doi.org/10.1002/2016rg000540

Thornton, J. A., Shilling, J. E., Shrivastava, M., D'Ambro, E. L., Zawadowicz, M. A., & Liu, J. (2020). A near-explicit mechanistic evaluation of isoprene photochemical secondary organic aerosol formation and evolution: Simulations of multiple chamber experiments with and without added NOx. *ACS Earth and Space Chemistry*, *4*(7), 1161–1181. https://doi.org/10.1021/acsearthspacechem.0c00118

Tsiligiannis, E., Hammes, J., Salvador, C. M., Mentel, T. F., & Hallquist, M. (2019). Effect of NOx on 1,3,5-trimethylbenzene (TMB) oxidation product distribution and particle formation. *Atmospheric Chemistry and Physics*, *19*(23), 15073–15086. https://doi.org/10.5194/acp-19-15073-2019

Vasquez, K. T., Crounse, J. D., Schulze, B. C., Bates, K. H., Teng, A. P., Xu, L., et al. (2020). Rapid hydrolysis of tertiary isoprene nitrate efficiently removes $NO_x$ from the atmosphere. *Proceedings of the National Academy of Sciences*, *117*(52), 33011–33016. 202017442. https://doi.org/10.1073/pnas.2017442117

Vereecken, L., Carlsson, P. T. M., Novelli, A., Bernard, F., Brown, S. S., Cho, C., et al. (2021). Theoretical and experimental study of peroxy and alkoxy radicals in the $NO_3$-initiated oxidation of isoprene. *Physical Chemistry Chemical Physics*, *23*(9), 5496–5515. https://doi.org/10.1039/D0CP06267G

Vereecken, L., & Peeters, J. (2009). Decomposition of substituted alkoxy radicals—Part I: A generalized structure–activity relationship for reaction barrier heights. *Physical Chemistry Chemical Physics*, *11*(40), 9062–9074. https://doi.org/10.1039/B909712K

Watne, A. K., Psichoudaki, M., Ljungstrom, E., Le Breton, M., Hallquist, M., Jerksjo, M., et al. (2018). Fresh and oxidized emissions from in-use Transit Buses running on Diesel, Biodiesel, and CNG. *Environmental Science and Technology*, *52*(14), 7720–7728. https://doi.org/10.1021/acs.est.8b01394

Wennberg, P. O., Bates, K. H., Crounse, J. D., Dodson, L. G., McVay, R. C., Mertens, L. A., et al. (2018). Gas-phase reactions of isoprene and its major oxidation products. *Chemical Reviews*, *118*(7), 3337–3390. https://doi.org/10.1021/acs.chemrev.7b00439

Wu, R., Vereecken, L., Tsiligiannis, E., Kang, S., Albrecht, S. R., Hantschke, L., et al. (2021). Molecular composition and volatility of multi-generation products formed from isoprene oxidation by nitrate radical. *Atmospheric Chemistry and Physics*, *21*(13), 10799–10824. https://doi.org/10.5194/acp-21-10799-2021

Xiong, F., Borca, C. H., Slipchenko, L. V., & Shepson, P. B. (2016). Photochemical degradation of isoprene-derived 4,1-nitrooxy enal. *Atmospheric Chemistry and Physics*, *16*(9), 5595–5610. https://doi.org/10.5194/acp-16-5595-2016

Xu, Z. N., Nie, W., Liu, Y. L., Sun, P., Huang, D. D., Yan, C., et al. (2021). Multifunctional products of isoprene oxidation in polluted atmosphere and their contribution to SOA. *Geophysical Research Letters*, *48*(1), e2020GL089276. https://doi.org/10.1029/2020GL089276

Ye, C., Yuan, B., Lin, Y., Wang, Z., Hu, W., Li, T., et al. (2021). Chemical characterization of oxygenated organic compounds in the gas phase and particle phase using iodide CIMS with FIGAERO in urban air. *Atmospheric Chemistry and Physics*, *21*(11), 8455–8478. https://doi.org/10.5194/acp-21-8455-2021

Zaveri, R. A., Shilling, J. E., Fast, J. D., & Springston, S. R. (2020). Efficient nighttime biogenic SOA formation in a polluted residual layer. *Journal of Geophysical Research: Atmospheres*, *125*(6), e2019JD031583. https://doi.org/10.1029/2019JD031583

Zhao, D., Pullinen, I., Fuchs, H., Schrade, S., Wu, R., Acir, I. H., et al. (2021). Highly oxygenated organic molecule (HOM) formation in the isoprene oxidation by $NO_3$ radical. *Atmospheric Chemistry and Physics*, *21*(12), 9681–9704. https://doi.org/10.5194/acp-21-9681-2021

## References From the Supporting Information

Albrecht, S. R., Novelli, A., Hofzumahaus, A., Kang, S., Baker, Y., Mentel, T., et al. (2019). Measurements of hydroperoxy radicals ($HO_2$) at atmospheric concentrations using bromide chemical ionisation mass spectrometry. *Atmospheric Measurement Techniques*, *12*(2), 891–902. https://doi.org/10.5194/amt-12-891-2019

Dörich, R., Eger, P., Lelieveld, J., & Crowley, J. N. (2021). Iodide CIMS and m/z 62: The detection of $HNO_3$ as $NO_3-$ in the presence of PAN, peroxyacetic acid and ozone. *Atmospheric Measurement Techniques*, *14*(8), 5319–5332. https://doi.org/10.5194/amt-14-5319-2021

Faxon, C., Hammes, J., Le Breton, M., Pathak, R. K., & Hallquist, M. (2018). Characterization of organic nitrate constituents of secondary organic aerosol (SOA) from nitrate-radical-initiated oxidation of limonene using high-resolution chemical ionization mass spectrometry. *Atmospheric Chemistry and Physics*, *18*(8), 5467–5481. https://doi.org/10.5194/acp-18-5467-2018

Iyer, S., Lopez-Hilfiker, F., Lee, B. H., Thornton, J. A., & Kurten, T. (2016). Modeling the detection of organic and inorganic compounds using iodide-based chemical ionization. *The Journal of Physical Chemistry A*, *120*(4), 576–587. https://doi.org/10.1021/acs.jpca.5b09837

Jenkin, M. E., Valorso, R., Aumont, B., & Rickard, A. R. (2019). Estimation of rate coefficients and branching ratios for reactions of organic peroxy radicals for use in automated mechanism construction. *Atmospheric Chemistry and Physics*, *19*(11), 7691–7717. https://doi.org/10.5194/acp-19-7691-2019

Kerdouci, J., Picquet-Varrault, B., & Doussin, J.-F. (2014). Structure–activity relationship for the gas-phase reactions of $NO_3$ radical with organic compounds: Update and extension to aldehydes. *Atmospheric Environment*, *84*, 363–372. https://doi.org/10.1016/j.atmosenv.2013.11.024

Lopez-Hilfiker, F. D., Mohr, C., Ehn, M., Rubach, F., Kleist, E., Wildt, J., et al. (2014). A novel method for online analysis of gas and particle composition: Description and evaluation of a filter inlet for gases and AEROsols (FIGAERO). *Atmospheric Measurement Techniques*, *7*(4), 983–1001. https://doi.org/10.5194/amt-7-983-2014

Vereecken, L., & Nozière, B. (2020). H migration in peroxy radicals under atmospheric conditions. *Atmospheric Chemistry and Physics*, *20*(12), 7429–7458. https://doi.org/10.5194/acp-20-7429-2020

Veres, P., Roberts, J. M., Warneke, C., Welsh-Bon, D., Zahniser, M., Herndon, S., et al. (2008). Development of negative-ion proton-transfer chemical-ionization mass spectrometry (NI-PT-CIMS) for the measurement of gas-phase organic acids in the atmosphere. *International Journal of Mass Spectrometry*, *274*(1–3), 48–55. https://doi.org/10.1016/j.ijms.2008.04.032

Zhang, W., & Zhang, H. (2021). Secondary ion chemistry mediated by ozone and acidic organic molecules in iodide-adduct chemical ionization mass spectrometry. *Analytical Chemistry*, *93*(24), 8595–8602. https://doi.org/10.1021/acs.analchem.1c01486